physica status solidi a
www.pss-a.com
applications and materials science

Synchrotron-radiation computed laminography for high-resolution three-dimensional imaging of flat devices

Lukas Helfen[1, 2], **Anton Myagotin**[1], **Alexander Rack**[1], **Petra Pernot**[1, 3], **Petr Mikulík**[4], **Marco Di Michiel**[3], and **Tilo Baumbach**[1, 2]

[1] ANKA/Institute for Synchrotron Radiation, Forschungszentrum Karlsruhe, Germany
[2] University of Karlsruhe, Germany
[3] European Synchrotron Radiation Facility, Grenoble, France
[4] Department of Condensed Matter Physics, Masaryk University, Brno, Czech Republic

Received 12 October 2006, revised 20 February 2007, accepted 16 May 2007
Published online 1 August 2007

PACS 07.05.Tp, 07.85.Qe, 87.59.–e

Synchrotron-radiation computed laminography (SRCL) is developed as a method for high-resolution three-dimensional (3D) imaging of regions of interest (ROIs) in all kinds of laterally extended devices. One of the application targets is the 3D X-ray inspection of microsystems. In comparison to computed tomography (CT), the method is based on the inclination of the tomographic axis with respect to the incident X-ray beam by a defined angle. With the microsystem aligned roughly perpendicular to the rotation axis, the integral X-ray transmission on the two-dimensional (2D) detector does not change exceedingly during the scan. In consequence, the integrity of laterally extended devices can be preserved, what distinguishes SRCL from CT where ROIs have to be destructively extracted (e.g. by cutting out a sample) before being imaged. The potential of the method for three-dimensional imaging of microsystem devices will be demonstrated by examples of flip-chip bonded and wire-bonded devices.

phys. stat. sol. (a) **204**, No. 8, 2760–2765 (2007) / **DOI** 10.1002/pssa.200775676

physica status solidi a

phys. stat. sol. (a) **204**, No. 8, 2760–2765 (2007) / **DOI** 10.1002/pssa.200775676

Synchrotron-radiation computed laminography for high-resolution three-dimensional imaging of flat devices

Lukas Helfen[*, 1, 2], **Anton Myagotin**[1], **Alexander Rack**[1], **Petra Pernot**[1, 3], **Petr Mikulík**[4], **Marco Di Michiel**[3], and **Tilo Baumbach**[1, 2]

[1] ANKA/Institute for Synchrotron Radiation, Forschungszentrum Karlsruhe, Germany
[2] University of Karlsruhe, Germany
[3] European Synchrotron Radiation Facility, Grenoble, France
[4] Department of Condensed Matter Physics, Masaryk University, Brno, Czech Republic

Received 12 October 2006, revised 20 February 2007, accepted 16 May 2007
Published online 1 August 2007

PACS 07.05.Tp, 07.85.Qe, 87.59.–e

Synchrotron-radiation computed laminography (SRCL) is developed as a method for high-resolution three-dimensional (3D) imaging of regions of interest (ROIs) in all kinds of laterally extended devices. One of the application targets is the 3D X-ray inspection of microsystems. In comparison to computed tomography (CT), the method is based on the inclination of the tomographic axis with respect to the incident X-ray beam by a defined angle. With the microsystem aligned roughly perpendicular to the rotation axis, the integral X-ray transmission on the two-dimensional (2D) detector does not change exceedingly during the scan. In consequence, the integrity of laterally extended devices can be preserved, what distinguishes SRCL from CT where ROIs have to be destructively extracted (e.g. by cutting out a sample) before being imaged. The potential of the method for three-dimensional imaging of microsystem devices will be demonstrated by examples of flip-chip bonded and wire-bonded devices.

1 Introduction

X-ray computed tomography (CT) is an established technique at synchrotron-radiation (SR) imaging setups for three-dimensional (3D) imaging of specimens or material samples. In general, CT is best applicable to specimens whose (integral) X-ray transmission does not change exceedingly during rotational scanning, e.g. as provided by cylindrically shaped specimens under rotation around their longitudinal axis.

SR-CT is currently being developed towards increased spatial resolutions [1, 2]. One drawback consists in the fact that, for a fixed number of pixels, the field of view of the detector (and therefore the spatial extensions of the specimen to be imaged) becomes reduced. Consequently, a sample has to be cut out at the region of interest (ROI), fitted to the field of view [1]. This means that high-resolution CT, as intrinsically non-destructive method, does not allow non-destructive quality inspection of devices exceeding the field of view. Moreover, imaging laterally extended specimens suffers from a large variation of the beam transmission while rotating the specimen in a CT experiment, leading to imaging artefacts. For instance, in the case of flat specimens (e.g. on planar substrates), the X-ray absorption is maximal in the directions parallel to the lateral specimen elongation. In combination with highly absorbing materials, X-ray transmission is negligible and hence no information is available from these projections.

[*] Corresponding author: e-mail: helfen@esrf.fr, lukas.helfen@iss.fzk.de, Phone: +33 476 88 2558, Fax: +33 476 88 2252

To overcome these limitations, synchrotron-radiation computed laminography (SRCL) was developed and successfully implemented for the first time [3] for high-resolution non-destructive 3D imaging of regions of interest (ROIs) in laterally extended specimens and devices (such as sensors, flip-chip devices and other microsystems). The scope of this paper is to present results recently obtained on the application field of microsystem device inspection. In comparison to its laboratory counterparts, synchrotron radiation provides specific advantages already exploited by radiography and tomography. For instance, monochromatic radiation of tunable X-ray energy is available in order to avoid beam hardening artefacts, or to select absorption edges of specific chemical elements in the specimen. Moreover, high beam intensity allows achieving high spatial resolutions at high signal-to-noise ratios even with monochromatic radiation. Furthermore, partial spatial coherence of the wavefield at the specimen position can be exploited for phase contrast and computer-holographic techniques after free-space propagation [4–6].

In order to make these advantages available to laminographic methods, the scanning geometry and 3D reconstruction has to account for particular experimental conditions of synchrotron imaging set-ups (such as a non-mobile source and a parallel beam). In the following section, the scanning scheme of SRCL will be introduced and its choice motivated. In Section 3, the potential of the method is highlighted by different applications to microelectronics and microsystem technology.

2 Methods

The basic principles were already proposed in 1932 – long before the development of CT – by Ziedses des Plantes [7]. Nowadays termed *classical X-ray tomography*, the method relied on the integration of the two-dimensional (2D) X-ray transmission during the scanning movements. At the time, it could be used to image few specific cross sections of specimens (or patients). To obtain large 3D images with a multitude of slices, however, a time-consuming translational scanning of the specimen with respect to the focal plane would have to be performed. By combining digital projection data and computerised reconstruction [8], the scanning procedure can now be avoided. The resulting method, called digital tomosynthesis, has analogy to CT with limited angle access. Due to the introduction of fast 2D digital detector systems and the tremendous increase of computing power the methods have recently found renewed interest in medical [8, 9] and technical [10, 11] applications.

The scanning scheme chosen for SRCL consists in the acquisition of projection data sets similar to standard CT, but with a rotation axis that is inclined at an angle $\theta < \pi/2$ instead of being perpendicular ($\theta = \pi/2$) to the incident beam in case of standard CT (see Fig. 1). If the device normal is aligned approximately parallel to the rotation axis, the integral X-ray transmission onto the 2D detector does not change considerably during specimen rotation and in particular avoids projections with missing information where the integral transmission would tend to zero due to a long beam path within the specimen.

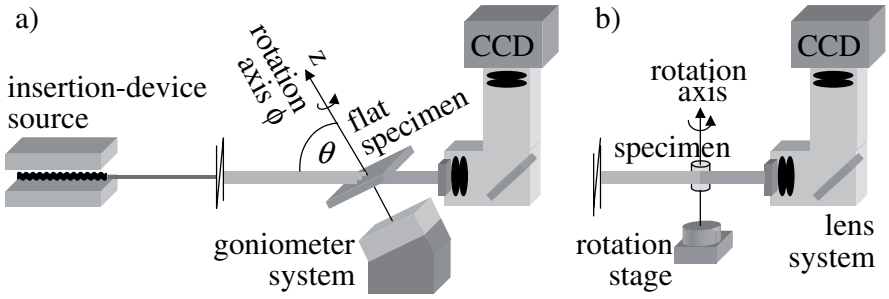

Fig. 1 (online colour at: www.pss-a.com) Comparison of the experimental set-ups for SRCL (a) and for SR-CT (b), as implemented at beamline ID15 of the ESRF.

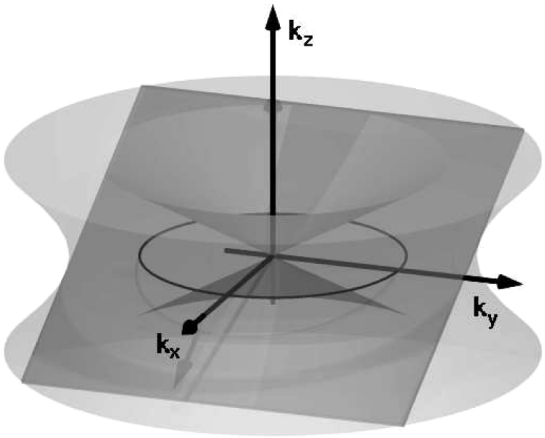

Fig. 2 Sampled region for the parallel-beam case in the 3D Fourier domain: the k_z is the Fourier conjugate to the z direction of the specimen coordinate system which is defined parallel to the laminographic rotation axis (see Fig. 1). The dark grey plane corresponds to the information gathered by a single 2D projection and is perpendicular to the direction of the incident beam. The region sampled by the entire scan is shown in lighter grey. It is a rotation-symmetric body where two cones along the positive and negative k_z directions are missing.

In general for all laminography methods, the 3D Fourier domain is not sampled completely. In comparison to CT there exist unsampled regions which, quite generally, may lead to artefacts in the reconstructed images. For the parallel-beam case, according to the projection-slice theorem generalised to three spatial dimensions [8], the region of the 3D Fourier domain sampled by a single 2D projection fills a plane perpendicular to the direction of the transmitted beam and passing through the origin of the 3D Fourier domain, see Fig. 2. Changing the specimen rotation angle ϕ (cf. Fig. 1) during the scan corresponds to turning this plane in the 3D Fourier domain around the k_z axis. Thus, for a large (evenly spaced) number of projections acquired onto an interval $0 \le \phi < 2\pi$, the sampled region corresponds to a rotation-symmetric body (light grey in Fig. 2) where two upwards and downwards directed inner cones of opening angle $2 \cdot (\pi - \theta)$ contain no experimental information.

The advantage of CL with circular scanning is an isotropic sampling of the in-plane components of laterally extended specimens. CT performed at such specimens (and in combination with highly absorbing materials) leads to the limitation of the angular range available for data acquisition since X-ray transmission is highly varying and approaching zero in a range of directions (e.g. almost parallel to the substrate). This leads to a highly anisotropic sampling of the 3D Fourier domain: the resolution of specimen features in the x,y-plane depends on their angular arrangements around the rotation axis.

The 3D reconstruction is performed by backprojection of filtered projections, according to scanning geometry. The filtering applied to the 2D projections yields an approximate inversion of the 3D modulation transfer function (MTF) of the combined process of projection and simple (unfiltered) backprojection [9]. Due to the missing information in the unsampled regions of the 3D Fourier domain (cf. Fig. 2), in general, exact inversion of the MTF is not possible which manifests itself in characteristic laminographic artefacts. Nevertheless, filtering of the 2D projection data minimises the artefacts in the reconstructed image.

3 Results

Simulations and test experiments have been carried out to demonstrate the feasibility of SRCL [3]. Moreover, the technological potential of SRCL for high-resolution non-destructive applications has been demonstrated [12].

A general problem in microsystem technology is the non-destructive inspection of hidden structures which are not accessible by visual inspection methods. The example presented in Fig. 3 illustrates the capabilities for 3D imaging of flip-chip bonded devices. There, after bump bonding, the flip-chip solder joints are not accessible by visual inspection anymore since they are enclosed between substrate and the integrated circuit (IC). Adapted to the rather highly absorbing bump materials, white radiation at an X-ray energy range between approximately 40 and 60 keV was used for the acquisition of 1800 angu-

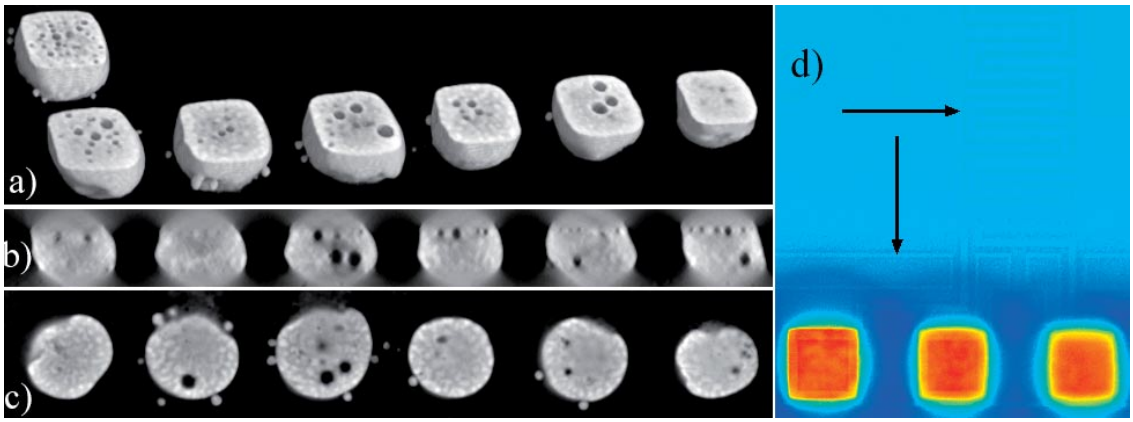

Fig. 3 (online colour at: www.pss-a.com) Inspection of a flip-chip bonded device by SRCL. The 3D data set rendered in (a) was reconstructed from 1800 projections (pixel size 1.6 μm) at an axis inclination of $\theta = \pi/3$ using an X-ray energy range between approx. 30 keV and 50 keV. The cross-sectional slice (b) is taken perpendicular to the substrate while slices (c) and (d) of the 3D data set are oriented parallel to the substrate and IC. Slice (d) features a detail of metallisation layers and conduction lines (see arrows) on the hidden surface of the IC.

larly equidistant projections of which a 3D data set was reconstructed. Image (a) shows a 3D rendition of bump bonds, cut open by a plane parallel to the substrate. Voids are clearly visible in the interior of the bump bonds. Such voids affect the long-term reliability of the device when it is exposed to heating/cooling cycles, e.g. due to device operation. Images (b) and (c) are reconstructed cross-sectional slices showing a number of large voids and smaller voids, the latter predominantly at the interface to the IC's metallisation layers (top part in b). Also, the Pb-rich phase of the solder is well visible (lighter grey scales) in slice (c), furthermore solder splashes near the bump bonds (small satellite spots). Slice (d) highlights a detail of the metallisations and conduction lines (see arrows) on the IC surface towards the bonding/substrate side.

Due to missing information in projections related to insufficient X-ray transmission, imaging of printed circuit boards (PCBs) by CT commonly introduces artefacts in the reconstructed slices. In the selected example of a wire-bonded IC protected by a glob top, see Fig. 4, the CT-reconstructed data set (a and b) features artefacts around the bond wires (15 μm diameter) which make the wires appear triangular in cross section. The data set reconstructed by CL (images c and e) was obtained with a similar lateral field of view of approximately 10 mm of the 2D detector system (1024 pixels of 10 μm size). We see that the triangular wire cross sections found for the CT measurements are not visible here. Especially from the 3D rendition (e) we see that the wire arrangement can be very well investigated including the bonding regions. Moreover, it allows one to distinguish between the highly absorbing (lighter) Au bond wires and the Cu circuit lines (darker) on the PCB. Furthermore, CL even allows increasing the spatial resolution of the detector system which is associated (for equal number of pixels) with a decrease of the lateral field of view. The example of images (d) and (f) with a reduced field of view of approximately 1.6 mm allows "zooming into" elements and structures, here the bonding pads on the surface of the IC (lower region in d). Please note, that the reduction of the imaged volume at a given ROI is *not* associated with a noticeable increase of artefacts.

A dedicated laminography set-up is developed by the University of Karlsruhe in cooperation with ANKA and the german Fraunhofer Society. It is installed at ESRF's imaging beamline ID19 in autumn 2006. Laterally large specimen can be handled efficiently without compromising the spatial resolution available from the detector systems. The instrument has been designed to be compatible also with ESRF's high-energy beamline ID15 so that highly absorbing specimens can be scanned with high throughput.

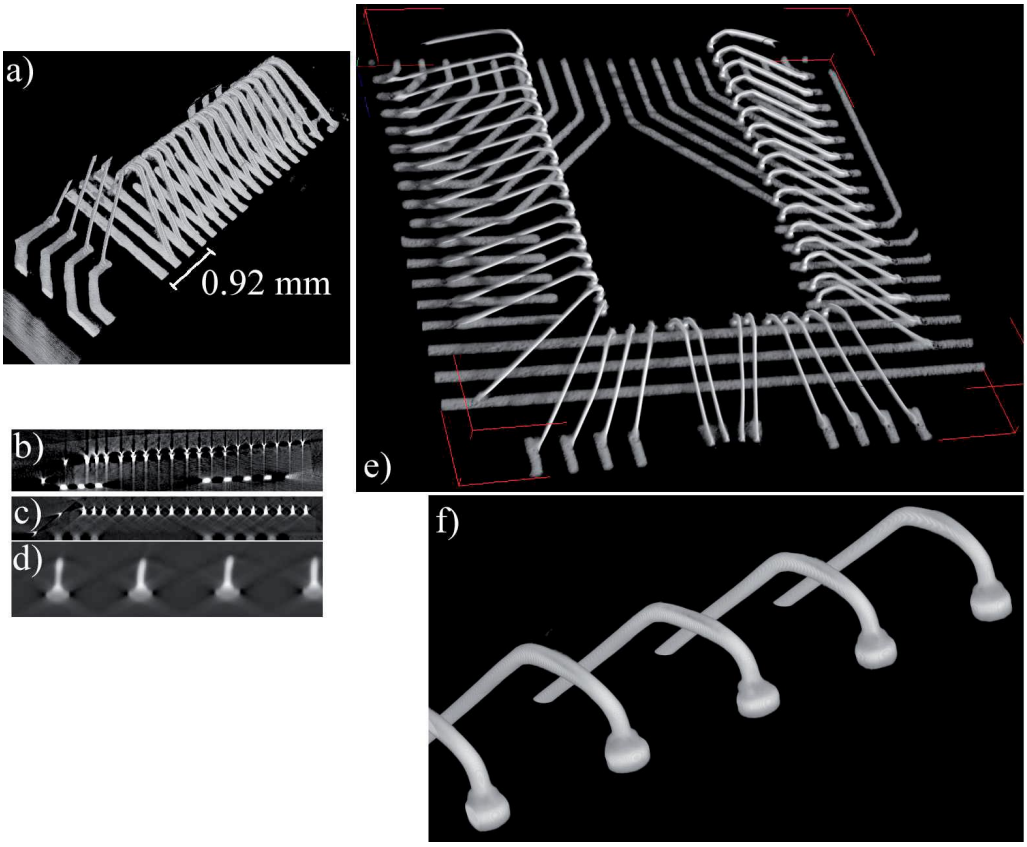

Fig. 4 Synchrotron X-ray inspection of an integrated circuit which is wire-bonded to a printed circuit board (PCB) and encapsulated within a glob top. Images (a, b) are performed by CT, images (c–f) by CL. For CL, images (c, e) performed with 10 μm pixel size serve for comparison with the CT data while images (d, f) illustrate imaging of an ROI with reduced field of view and higher spatial resolution of 1.6 μm pixel size.

4 Summary

The reported results of simulations and experiments demonstrate the potential of synchrotron-radiation computed laminography. It provides a unique tool for non-destructive imaging of flat, laterally extended specimens with spatial resolutions presently down to the μm scale. The potential of the method is highlighted by the image quality obtained.

A dedicated laminography set-up will be commissioned at ESRF's imaging beamline ID19 during autumn 2006. It will allow efficient scanning of large laterally extended specimens with sizes up to $150 \times 150 \times 5$ mm^3. First user experiments are planned from spring 2007 onwards. One of the application fields aimed at is research and development in microsystem technology – encompassing the design, processing, production and application of technical systems which by miniaturisation of their components contain critical structural sizes down to the (sub-)μm scale integrated in devices of macroscopic dimensions.

Acknowledgements This work was supported by an ESRF long-term project. The authors acknowledge R. Chagnon, W. Schmid and D. Fernandez Carreiras for their contributions to the experimental set-up. P. Mikulík acknowledges support by the Ministry of Education of the Czech Republic (Grant MSM 0021622410). The implementation of the laminography instrument is part of a cooperation contract with ANKA at Forschungszentrum Karlsruhe and the Fraunhofer Institute for Nondestructive Testing, Saarbrücken/Dresden, Germany.

References

[1] C. Schroer, M. Meyer, M. Kuhlmann, B. Benner, T. Günzler, B. Lengeler, C. Rau, T. Weitkamp, A. Snigirev, and I. Snigireva, Appl. Phys. Lett. **81**, 1527–1529 (2002).
[2] M. Stampanoni, G. Borchert, R. Abela, and P. Rüegsegger, Appl. Phys. Lett. **82**, 2922–2924 (2003).
[3] L. Helfen, T. Baumbach, P. Mikulík, D. Kiel, P. Pernot, P. Cloetens, and J. Baruchel, Appl. Phys. Lett. **86**, 071915 (2005).
[4] K. A. Nugent, T. E. Gureyev, D. F. Cookson, D. Paganin, and Z. Barnea, Phys. Rev. Lett. **77**, 2961–2964 (1996).
[5] P. Cloetens, W. Ludwig, J. Baruchel, D. van Dyck, J. van Landuyt, J. Guigay, and M. Schlenker, Appl. Phys. Lett. **75**, 2912 (1999).
[6] T. E. Gureyev, C. Raven, A. Snigirev, I. Snigireva, and S. W. Wilkins, J. Phys. D **32**, 563–567 (1999).
[7] B. G. Ziedses des Plantes, Acta Radiol. **13**, 182–192 (1932).
[8] J. T. Dobbins III and D. J. Godfrey, Phys. Med. Biol. **48**, R65–R106 (2003).
[9] G. Lauritsch and W. H. Härer, Proc. SPIE **3338**, 1127–1137 (1999).
[10] J. Zhou, M. Maisl, H. Reiter, and W. Arnold, Appl. Phys. Lett. **68**(24), 3500–3502 (1996).
[11] S. Gondrom, J. Zhou, M. Maisl, H. Reiter, M. Kröning, and W. Arnold, Nucl. Eng. Des. **190**, 141–147 (1999).
[12] L. Helfen, A. Myagotin, P. Pernot, M. DiMichiel, P. Mikulík, A. Berthold, and T. Baumbach, Nucl. Instrum. Methods A **563**, 163–166 (2006).

